















Figure 7. Generator temperature as a function of COP for different evaporator temperatures.

Analyzing the behavior of Fig. 7, it is noticed that the higher evaporator temperature showed higher COP values, ranging between 0.37 and 0.61. For lower temperatures, as in  $T_7 = -5$  °C the COP varied between 0.36 and 0.59. When the ammonia vapor leaving the evaporator has higher temperatures, this indicates that there has been a greater heat transfer from the fluid to be cooled to the evaporator, that is, the greater the amount of heat removed from the fluid to be cooled so that the ammonia evaporates, consequently increasing the performance of the system.

For analysis of the Influence of pressure at the outlet of the absorber ( $P_1$ ) on the COP of the system, the temperature of the generator  $T_3$  was varied as a function of the COP of the system for different types of pressure  $P_1$ . With this, it was possible to investigate the impact of this parameter on the overall performance of the system. As initial parameters of model for this case, was defined as absorber temperature  $T_3 = 20$  °C and for condenser temperature  $T_5 = 20$  °C. The result of applying these parameters are shown in Fig. 8.

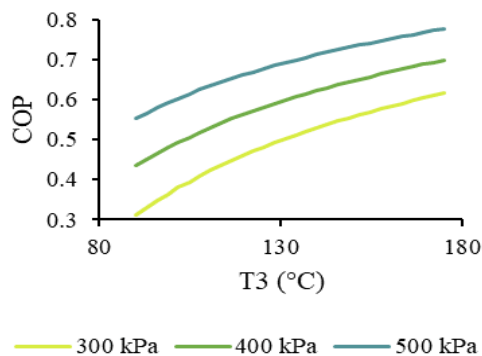


Figure 8. Generator temperature as a function of COP for different pressures.

Through Fig. 8, it is observed that the higher the value of the saturation pressure of the evaporator  $P_1$ , the higher the COP of the system, where for the pressure  $P_1 = 500$  kPa, COP values between 0.55 and 0.77 were obtained. In this case, higher values of  $P_1$  imply higher temperatures of the fluid at the outlet of the evaporator, that is, a greater amount of heat transfer was required from the fluid to be cooled to the evaporator. That is, the higher the pressure  $P_1$  in the evaporator, the greater the amount of heat needed to evaporate the ammonia, increasing the efficiency of the cycle. Furthermore, the pressure  $P_1$  it also influences the amount of ammonia that is dissolved in the water in the absorber. Greater values of  $P_1$  imply higher amounts of ammonia mass fraction leaving the evaporator.

It is also important to mention that the greater the value of  $P_3$ , the greater the value of the specific volume of the liquid solution that leaves the evaporator and, consequently, the greater the drive power required by the pump. However, the mixture that passes through the pump is a liquid solution of  $NH_3 \cdot H_2O$ , presenting much smaller values of specific volume if compared to the ammonia vapor. For this reason, the pump drive power for this type of refrigeration system is very low, having no relevant impact on the COP of the system. To prove this fact from the model developed, another value was calculated for the COP of the system, which does not take into account the power of the pump. Then, the temperature of the generator was varied  $T_3$  as a function of the two performance coefficients, where  $COP_1$  considers the pump power and  $COP_2$  does not. The result of such an analysis is shown in Fig. 9

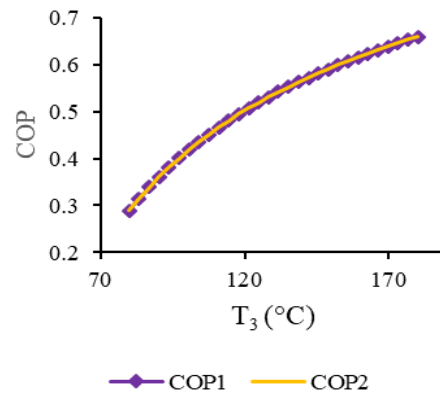


Figure 9. Effect of pump power on system COP.

As expected, there is no relevant difference when considering the pump drive power or not in the performance calculations of refrigeration systems by absorption.

The amount of ammonia mass fraction of the vapor leaving the generator/rectifier is an important factor in the cycle. Some absorption refrigeration cycles use a rectifier before the condenser precisely to remove any liquid existing in the fluid, causing only ammonia vapor to enter the condenser. In the mathematical model developed, this is represented by the fraction of dough at point 4 ( $x_4$ ). To analyze the relevance that this property has on performance of the system, varied  $x_4$  depending on the COP. The behavior obtained is shown in Fig 10.



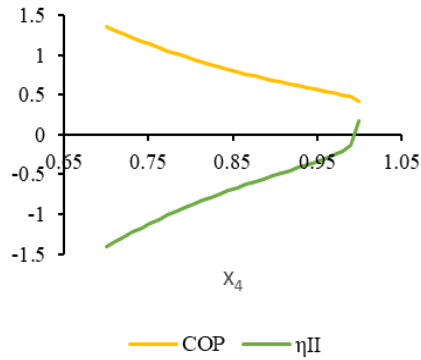


Figure 10. Influence of  $x_4$  on system performance.

Through Fig. 10, it can be seen that the system has higher COP values when the ammonia mass fraction is further away from the unit. However, also plotting the exergetic efficiency curve, it is seen that for  $x_4$  values lower than approximately 0.9995, the system presented negative exergetic efficiency, that is, the system loses more energy than the amount that enters the system, making the system impracticable.

For analyze the influence of the fluid temperature at the output of the generator  $T_3$  in relation to the exergetic efficiency of the system, a pressure  $P_1 = 350$  kPa and the temperatures of the absorber and condenser of  $T_1 = T_5 = 30^\circ\text{C}$  were chosen as input parameters. Furthermore, it was considered that 10 kW is constantly supplied to the generator ( $Q_G = 10\text{kW}$ ). The behavior of the exergetic efficiency of the system as a function of generator temperature is shown in Fig. 11.

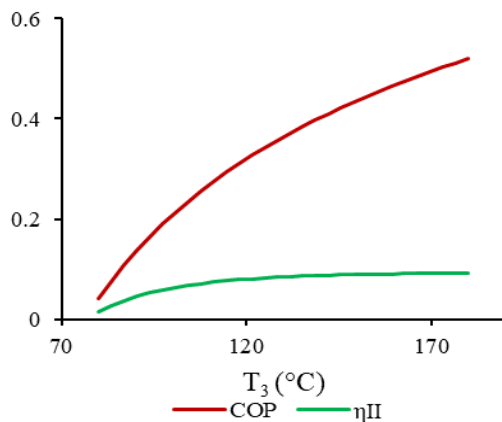


Figure 11.  $T_3$  as a function of COP and exergetic efficiency.

From the behavior obtained in Fig. 11, it is noted that the higher the temperature  $T_3$ , the higher the corresponding value of the COP of the system.

However, in relation to exergetic efficiency, even if higher values of  $T_3$  result in a greater amount of steam of ammonia in the generator, there is also an increase in exergy losses both in the generator and in the absorber, reducing the exergetic efficiency of the system. It can be seen that from approximately  $T_3 = 140^\circ\text{C}$ , there is no significant variation in the second law efficiency, even for higher values of  $T_3$ , precisely due to the increase in exergy losses caused by the increase in temperature in this component. This increase in the destruction of exergy in the generator/rectifier as a function of the increase in temperature  $T_3$  is shown in Fig. 12, where it can be seen that from approximately  $112^\circ\text{C}$  the destruction of exergy in this component increases significantly.

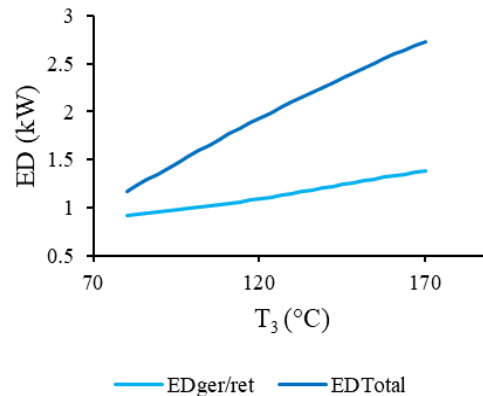


Figure 12.  $T_3$  as a function of the exergy destroyed in the generator/rectifier and the total destroyed exergy of the system.

With this, it can be said that only a first law analysis, that is, through the behavior of the COP as a function of the generator/rectifier temperature, is not enough to correctly analyze the performance of a refrigeration system. It is also necessary to take into account, for a more consistent analysis, the rate of exergy destruction in each component and the exergetic efficiency of the system.

For obtain the influence of  $T_1$  on the second law efficiency,  $P_1 = 500$  kPa,  $T_5 = 25^\circ\text{C}$  was used as input parameters, and the heat transfer  $Q_G$  was kept constant for all cases in this section. The behavior obtained is shown in Figure 13, where the temperature of the generator  $T_3$  was varied as a function of the exergetic efficiency for three values of temperature of the absorber  $T_1$ .

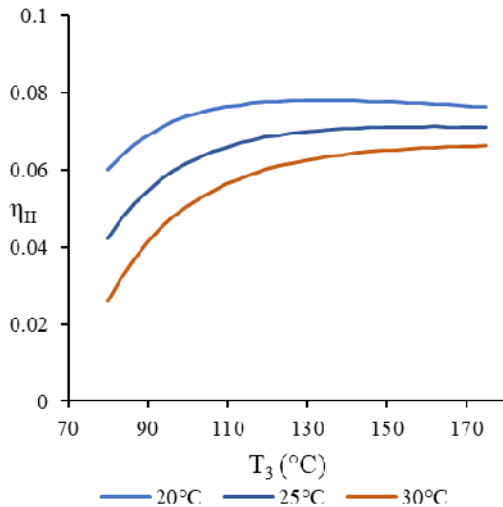


Figure 13.  $T_3$  as a function of exergetic efficiency for different temperature values of the  $T_1$  absorber.

From Figure 13, it is observed that the lower the absorber temperature, the higher the exergetic efficiency of the system, where for a temperature  $T_1 = 20\text{ }^\circ\text{C}$  the second law efficiency presented values between 0.0599 and 0.0762. This is explained by the fact that higher heat transfer in the evaporator results in higher temperature ammonia vapor entering the absorber. Thus, there is a greater heat transfer from the absorber for cooling water in this component so that the temperature of the mixture at the outlet of the absorber is decreased since in this component the temperature of the solution is inversely proportional to the amount of ammonia that can be dissolved in the water. Regarding the temperature of condenser  $T_5$ , the following values were used as input parameters:  $P_1 = 300\text{ kPa}$  and  $T_1 = 30\text{ }^\circ\text{C}$ . With these parameters and varying the temperature of  $T_3$  as a function of the exergetic efficiency, for different temperatures of  $T_5$ , the behavior is obtained as shown in Figure 14.

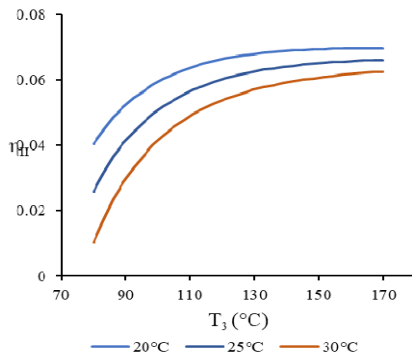


Figure 14.  $T_3$  as a function of exergetic efficiency for different condenser temperatures  $T_5$

Analyzing the behavior of the curves in Figure 14, it can be seen that the system presented higher values of exergetic efficiencies for lower values of condenser  $T_5$  temperature, with values ranging between 0.0403 and 0.0691 for  $T_5 = 20\text{ }^\circ\text{C}$ . This is because higher condenser temperatures result in lower evaporator heat transfer rates as the liquid leaving the condenser will be at a higher temperature. Lower values for condenser temperature imply greater heat transfer in the evaporator, increasing the exergetic efficiency of the system. For analyze the influence of  $T_7$  on exergetic efficiency,  $P_1 = 300\text{ kPa}$ ,  $T_1 = 30\text{ }^\circ\text{C}$  and  $T_5 = 25\text{ }^\circ\text{C}$  were used as input parameters. The temperature of generator  $T_3$  was then varied as a function of the exergetic efficiency of the system for different  $T_7$  evaporator temperatures, as shown in Figure 15.

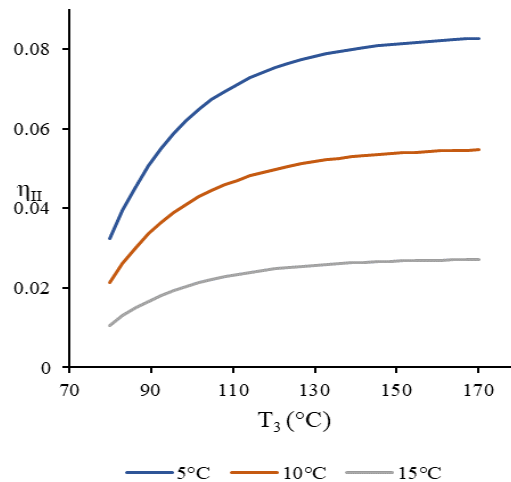


Figure 15.  $T_3$  as a function of exergetic efficiency for different temperatures of the  $T_7$  evaporator.

Analyzing Figure 15, it can be seen that the system has higher exergetic efficiency values when the temperature of the  $T_7$  evaporator is lower, where the second law efficiency varied between 0.032 and 0.082 for  $T_7 = 5\text{ }^\circ\text{C}$  and between 0.021 and 0.055 for  $T_7 = 10\text{ }^\circ\text{C}$ . In the evaporator, lowering  $T_7$  temperature has a greater impact on exergetic efficiency than increasing heat transfer  $Q_E$ . That is, the evaporator has greater cooling potential at lower temperatures.

The temperature in the generator  $T_3$  was varied as a function of the exergetic efficiency for different values of heat transfer to the generator, as shown in Figure 16. The input parameters defined were  $P_1 = 300\text{ kPa}$ ,  $T_1 = 20\text{ }^\circ\text{C}$  and  $T_5 = 25\text{ }^\circ\text{C}$ .

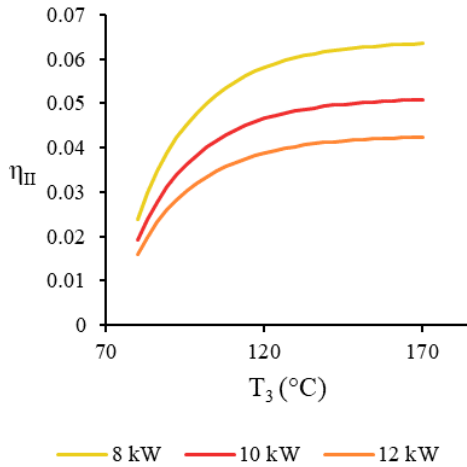


Figure 16.  $T_3$  as a function of exergetic efficiency for different  $Q_G$  values.

Through the analysis of Figure 16, lower values of second law efficiency are observed for smaller values of  $Q_G$ , where for this case it presented values between 0.024 and 0.063 for  $Q_G = 8\text{ kW}$  and for  $Q_G = 10\text{ kW}$  it presented values between 0.019 and 0.051. This happens because the more heat is supplied to the generator, the higher the temperature  $T_3$  and the greater the exergy losses associated with both the generator and the absorber and condenser, reducing the exergy efficiency of the system.

For assessing the amount of exergy destroyed in each component, the input parameters in the model described in Table 03 were used. Applying Eqs. 19 – 25, the behavior illustrated in Figure 17 was obtained.

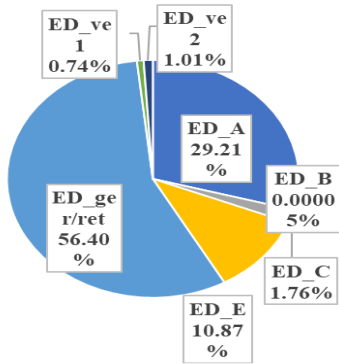


Figure 17. Share of exergy destruction of each component of the absorption refrigeration cycle.

The components that showed the highest rate of exergy destruction were the generator/rectifier set and the absorber, with 56.4% and 29.2%, respectively, of the total exergy destroyed in the system. These irreversibilities occur mainly due to the mixing process with greater temperature differences that takes place in these components. Knowing this, in

terms of design improvement and optimization, these two components would require more attention in order to decrease the amount of total system exergy destruction, thus improving system performance.

In order to improve the performance of the refrigeration system model as a function of parameters such as temperature and pressure, values were sought to present exergetic efficiency optimizations for certain operating conditions. To calculate the maximum or minimum values of the parameters of this work, the Golden Section Search method, available at EES, was used. According to Bagheri et al. (2019), this method is more consistent than the quadratic approximation method, also available through the software. In addition, temperature and pressure values were sought that minimize the destruction of exergy in the generator/rectifier, since which is the component with the highest exergy losses. For this, the Golden Section Search method, available at EES, was also applied.

Initially, a temperature value was sought in the  $T_3$  generator/rectifier that presented the highest exergetic efficiency with the input parameters described in Table 4.

Table 4. Model input parameters for exergetic optimization as a function of  $T_3$ .

Parameters	Symbol	Unit	Value
Pump Mass Flow		kg/s	0.01
Pressure at the outlet of the absorber		kPa	300
Absorber Temperature		°C	20
Condenser Temperature		°C	20
Heat transfer to the generator		kW	10
Mass fraction of ammonia at the generator/rectifier output		-	0.9996

Thus,  $T_3$  is varied as a function of the second law efficiency in order to seek an optimal temperature value which results in the highest exergetic efficiency for these operating conditions, as shown in Figure 18.

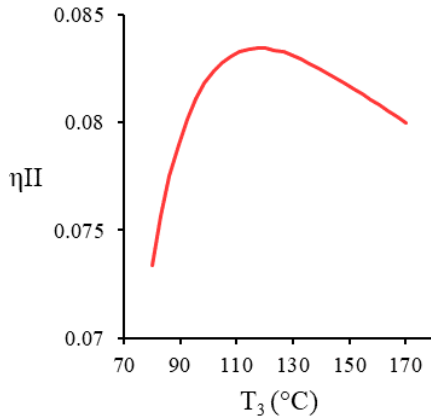


Figure 18. Exergetic optimization as a function of  $T_3$  generator/rectifier temperature.

Note that the exergetic efficiency has an increasing behavior up to a certain temperature value and then starts to decrease with the increase of  $T_3$ . Therefore, it is possible to obtain a temperature value  $T_3$  in which the system will present a value optimal exergetic efficiency. The values that optimize the model for this case were  $T_3 = 118.2^\circ\text{C}$  with an exergetic efficiency of 0.08344.

Optimization as a function of  $P_1$ , it was also sought, values of pressure  $P_1$  that resulted in greater exergetic efficiency in the developed model of cooling system. For this case, the input parameters described in Table 5 were used.

Table 5. Model input parameters for exergetic optimization as a function of  $P_1$ .

Parameters	Symbol	Unit	Value
Pump Mass Flow		kg/s	0.01
Condenser Temperature	$T_5$	$^\circ\text{C}$	30
Absorber Temperature	$T_1$	$^\circ\text{C}$	30
Heat transfer to the generator		kW	5
Mass fraction of ammonia at the generator/rectifier output	$x_4$	-	0.9996

Varying  $P_1$  as a function of the second law efficiency, the behavior shown in Figure 19 is obtained.

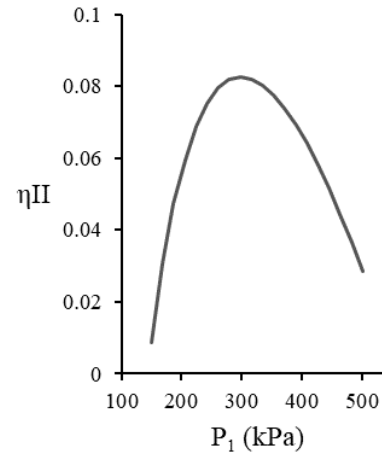


Figure 19. Exergetic optimization as a function of pressure at the outlet of the absorber  $P_1$ .

Analyzing Figure 19, it can be seen that between pressures of 150 kPa and approximately 297 kPa, there is an increase in exergetic efficiency. By increasing the pressure value, a maximum value for efficiency is reached and then this is reduced as  $P_1$  increases. The reduction in efficiency occurs because the system pressure in the output of the absorber is the same saturation pressure of the evaporator, that is, the increase of  $P_1$  results in the increase of the temperature of the evaporator  $T_7$ , reducing the efficiency of second law. The optimal point found for this case was at  $P_1 = 298.5$  kPa and an exergetic efficiency of 0.08254.

Temperature and pressure values were obtained that minimize the exergy losses in the generator/rectifier, which was indicated by the exergy analysis as the component responsible for the greater destruction of exergy in the developed model. Minimizing this parameter is extremely important from the point of view of system performance, in which the generator/rectifier is the greatest source of irreversibility, as it presents a greater share of total system exergy destruction.

For this analysis, the input parameters shown in Table 6 were used, where the temperature of the  $T_1$  absorber was varied as a function of the exergy destroyed in the generator/rectifier, obtaining the behavior of Fig. 20.

Table 6. Model input parameters for calculating the minimum value of exergy destroyed in the generator/rectifier.

Parameters	Symbol	Unit	Value
Pump Mass Flow		kg/s	0.01
Condenser Temperature	T5	°C	30
Pressure at the outlet of the absorber	P1	°C	350
Heat transfer to the generator		kW	10
Mass fraction of ammonia at the generator/rectifier output	x4	-	0.9996

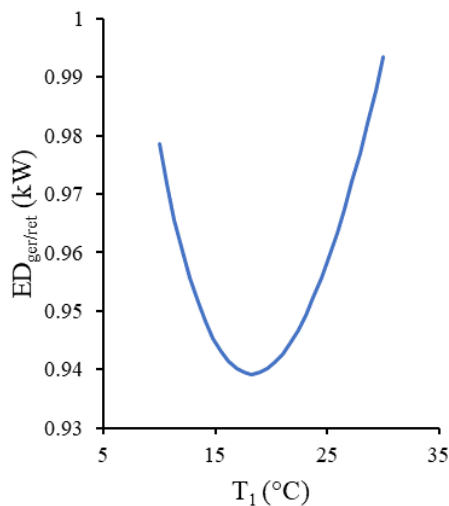


Figure 20. Reduction of exergy destroyed in the generator/rectifier as a function of absorber temperature.

From the behavior of the curve in Figure 20, it can be seen that there is a temperature value  $T_1$  where the value of exergy destruction in the generator/rectifier is the minimum possible. The minimum exergy destruction value obtained for this component was 0.9392 kW at  $T_1 = 18.3^\circ\text{C}$ . By increasing the temperature of the absorber, the destruction of the exergy of the generator/rectifier also has its value increased, because the temperature of the solution that leaves the absorber is at a higher temperature, increasing the mixing losses in the generator/rectifier. Furthermore, it can be affirmed through the analysis of Figure 20, that solutions with a high concentration of ammonia also generate a greater destruction of exergy in the generator/rectifier. This is represented in the graph

when the temperature values are less than  $18.3^\circ\text{C}$ . Thus, it can be seen that for  $T_1$  values  $<18.3^\circ\text{C}$ , the exergy destruction in the generator/rectifier increases, as well as the concentration of ammonia in the solution leaving the absorber. This occurs because the solution is making the absorber richer in ammonia, but at a low enough temperature to increase the losses in the generator/rectifier.

The minimum value of  $ED_{\text{ger/ret}}$  as a function of  $P_1$ . Pressure at the outlet of the  $P_1$  absorber was also analyzed as a function of the exergy destruction in the generator/rectifier. For this, the values from Table 08 were also used, considering  $T_1 = 20^\circ\text{C}$  and varying  $P_1$  as a function of the exergy destroyed in the generator/rectifier, presenting the behavior described in Figure 21.

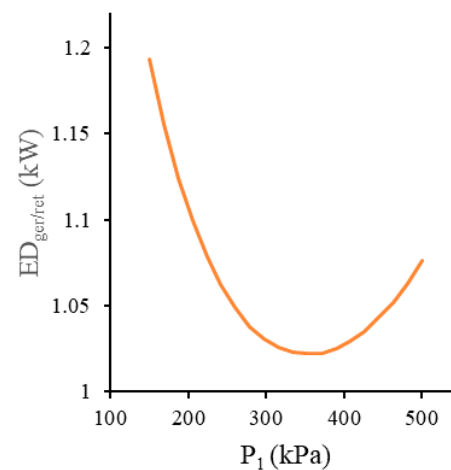


Figure 21. Reduction in the amount of exergy destroyed in the generator/rectifier as a function of the output pressure of the  $P_1$  absorber.

Applying the Golden Section Search through the EES, the value of  $P_1 = 353.5$  kPa was determined, for which the exergy destruction presented a minimum value of 1.021 kW for this case. The behavior of the curve shown in Figure 21 is explained by the fact that the higher  $P_1$ , the greater the absorption efficiency, that is, the greater the amount of ammonia in the solution that goes to the generator. However, the temperature of the absorber is constant, requiring greater heat transfer in the generator, increasing the losses in this component. And if the pressure drops below 353.5 kPa, the solution will get weaker and weaker in terms of ammonia concentration, also increasing the losses in the generator/rectifier.

## CONCLUSIONS

The main conclusions of this article are summarized according to the specific objectives of this work, i) A steady-state mathematical model of an absorption refrigerator was developed to represent the

operation of the main components of the refrigeration cycle as a function of the operating parameters, ii) The equation of the mathematical model using mass, energy and entropy balances was implemented in the Engineering Equation Solver (EES), iii) A parametric analysis of the system was performed, from which the importance of component temperatures as a function of COP and exergetic efficiency was studied. The impact of the pressure at the outlet of the absorber on the performance of the system was analyzed and also how the mass fraction of ammonia that enters the condenser must be greater than 0.9995, where values smaller than this resulted in negative exergetic efficiency of the system. In addition, the impact of the increase in temperature of the generator/rectifier on the destruction of exergy in the system was also shown, in which increasing this temperature increases the irreversible losses in this component, iv) An exergy analysis of the cooling system was also carried out, from which it was possible to assess that the generator/rectifier is responsible for approximately 56.4% of the total exergy destroyed in the system. Thus, the analysis indicated that the generator/rectifier is the most important component from the point of view of irreversibilities, with the greatest potential to improve system performance, v) and The exergetic optimization of the absorption refrigeration system was carried out under certain operating conditions, where an exergetic efficiency of 0.08344 was obtained for  $T_3 = 118.2$  °C, as well as an exergetic efficiency of 0.08254 for  $P_1 = 298.5$  kPa. The values of  $T_1$  and  $P_1$  were obtained that resulted in the lowest possible value of exergy destruction of the generator/rectifier in certain cases, where  $T_1 = 18.3$ °C presented  $ED_{\text{ger/ret}} = 0.9392$  kW and  $P_1 = 353.5$  kPa resulted in  $ED_{\text{ger/ret}} = 1.021$  kW.

#### ACKNOWLEDGEMENTS

The authors acknowledge with gratitude the support I would like to thank to the Brazilian National Council of Scientific and Technological Development, CNPq (projects 407198/2013-0, 403560/2013-6, 407204/2013-0, 430986/2016-5, 443823/2018-9, 313646/2020-1, 310708/2017-6, 308460/2020-0 and 446787/2020-5), CAPES, Ministry of Education, Brazil (projects 062/14 and CAPES-PRINT-UFPR-88881.311981/2018-01), and Araucaria Foundation of Parana, Brazil (project 115/2018, no. 50.579 – PRONEX).

#### REFERENCES

ADEWUSI, S. A. ZUBAIR, S. M. Second Law based Thermodynamic Analysis of Ammonia-Water Absorption Systems. *Energy Conversion and Management*, v. 45, p. 2355-2369, 2004.

EPE – EMPRESA DE PESQUISA ENERGÉTICA. Balanço Energético Nacional 2019: Ano Base 2018.

HEROLD, K. E.; RADERMACHER, R.; KLEIN, S.A. *Absorption Chillers and Heat Pumps*, CRC Press, Florida, 2016.

KIM, B. PARK, J. Dynamic Simulation of a Single-Effect Ammonia-Water Absorption Chiller. *International Journal of Refrigeration*, v. 30, p. 535-545, 2007.

MARTINEZ, L.C. Modelagem matemática quasi-permanente e simulação de componentes de refrigeradores por absorção, Dissertação de mestrado, Universidade Federal do Paraná, 2018.

MARTINHO, L. C. S. Modelagem, Simulação e Otimização de Refrigeradores por Absorção. Tese de Doutorado. Universidade Federal do Paraná, Curitiba, 2013.

STOECKER, W. F., JONES, J. W. *Refrigeração e Ar Condicionado*. São Paulo: McGraw Hill do Brasil LTDA, 1985.

U.S. Energy Information Administration. *Electric Power Monthly with data for January 2022*.

VARGAS, J. V. C. PARISE, J. A. R. LEDEZMA, G. A. BIANCHI, M. V. A. Thermodynamic Optimization of Heat-Driven Refrigerators in the Transient Regime. *Heat Transfer Engineering*, v. 25, p. 35-45, 2000.

ZIEGLER, F. Recent developments and future prospects of sorption heat pump systems. *Int. J. Therm. Sci.*, v. 38, p. 191-208, 1999.